Dynamic Reliability Kernels for Single-Valued Neutrosophic Evidence Fusion: A Mathematical Model for Multi-Source Market-State Classification

Samandarboy Sulaymanov[1,*], **Maha Ibrahim**[1]
[1]Tashkent state university of economics, Uzbekistan
Emails: sulaymanovsamandarboy@gmail.com ; maha.ahmed860@hgmail.com

Abstract

Multi-source decision systems require a representation in which supportive evidence, contradictory evidence, and weak evidence are not collapsed into the same numerical channel. This paper develops a dynamic reliability-kernel model for single-valued neutrosophic evidence fusion. Given a matrix of source signals, each source is transformed into a single-valued neutrosophic triplet whose truth, indeterminacy, and falsity memberships are governed by signed evidence strength. A time-varying reliability kernel then assigns larger mass to sources with lower recent instability, and a dispersion-augmented fusion operator produces a global neutrosophic state. The final decision rule is formulated as a penalized neutrosophic score and as a regularized probabilistic classifier over the fused triplet. The model is evaluated on a public weekly stock dataset containing six technology-market sources. The results show that the proposed representation achieves competitive chronological classification performance while providing explicit mathematical control over indeterminacy, disagreement, and reliability. Ablation and penalty-sensitivity analyses demonstrate that indeterminacy is a functional component of the decision model rather than a cosmetic label. The paper offers a reproducible mathematical framework for neutrosophic information fusion in uncertain intelligent decision-support systems.

Keywords: Single-valued neutrosophic sets; Neutrosophic evidence fusion; Reliability kernel; Indeterminacy penalty; Multi-source classification; Uncertainty-aware decision support

1. Introduction

Information-fusion systems often operate on evidence that is numerically available but epistemically incomplete. A sensor reading, financial indicator, medical measurement, or user-behavior signal may support a state, oppose it, or be too weak to justify either conclusion. Classical feature concatenation and probabilistic classification can model predictive uncertainty, but they usually do not preserve the difference between lack of evidence and negative evidence. This distinction is important in decision-support systems because a low-confidence positive state and a strongly negative state may require different actions.

Neutrosophic theory provides a direct mathematical language for this problem by representing an object through truth, indeterminacy, and falsity memberships. In a single-valued neutrosophic setting, each source is described by a triplet in $[0,1]^3$, allowing supportive, ambiguous, and contradictory evidence to coexist. When this representation is combined with information fusion, the decision model can aggregate evidence while retaining a measurable indeterminacy component. This is more expressive than mapping every source into a single probability or score.

The core question addressed in this paper is how to build a mathematically explicit neutrosophic fusion model for real multi-source data rather than using neutrosophic terminology only as a descriptive layer. The proposed answer is a dynamic reliability-kernel single-valued neutrosophic evidence fusion model. It starts from a signal matrix, maps each source to a single-valued neutrosophic triplet, estimates time-varying source reliability from recent instability, aggregates the triplets through a normalized kernel, and applies an indeterminacy-penalized decision function.

The empirical setting is multi-source market-state classification. The domain is useful for methodological evaluation because asset-level signals are correlated, volatile, and occasionally conflicting. The goal is not to design a trading rule; rather, the dataset provides a reproducible testbed in which six public sources jointly determine a binary future market state. The same formulation can be applied to sensor networks, medical screening, cyber-risk monitoring, and other fusion problems where signals have unequal reliability and ambiguous strength.

The main contributions are as follows. First, the paper formalizes a source-wise single-valued neutrosophic mapping from signed numerical evidence into truth, indeterminacy, and falsity memberships. Second, it defines a dynamic reliability kernel and proves boundedness and convex preservation of the fused triplet. Third, it introduces a

DOI: https://doi.org/10.54216/NIF.050102
Received: December 31, 2024 Accepted: February 28, 2025

Table 1: Summary of recent studies related to neutrosophic and information-fusion modeling.

Study	Venue	Focus	Main relevance
Meng et al. (2020)	Information Fusion	Machine-learning data fusion survey	Synthesized feature-, decision-, and hybrid-fusion paradigms
Chen et al. (2022)	Information Fusion	Public/expert opinion fusion	Modeled dynamic reliability in large-scale decision contexts
Zeng et al. (2022)	Electronics	SVNS similarity measure	Modified Manhattan similarity for pattern recognition and MADM
Farid and Riaz (2022)	Complex & Intelligent Systems	SVN aggregation	Einstein interactive aggregation for engineering selection
Wajid et al. (2023)	Journal of Intelligent & Fuzzy Systems	Neutrosophic CNN fusion	Image-text classification with neutrosophic uncertainty management
Farid and Riaz (2023)	Engineering Applications of AI	SVN dynamic aggregation	Time-sequence preferences for IoT supply-chain technology selection
Yang et al. (2024)	Artificial Intelligence Review	Multi-scale SVN decisions	Three-way decision and evidence theory for scale selection
Lavanya et al. (2024)	Applied Soft Computing	Neutrosophic image fusion	Neutrosophic entropy and feature extraction for multimodal images
Shaik et al. (2024)	Information Fusion	Multimodal healthcare fusion survey	Mapped fusion from data to knowledge and wisdom
Jiao and Pan (2024)	Entropy	Uncertain information fusion	Approximate reasoning and uncertainty handling in fusion systems

dispersion-augmented indeterminacy term and a penalized decision score that explicitly controls the effect of ambiguous evidence. Fourth, it reports real numerical results on a public dataset and evaluates the contribution of the neutrosophic components through ablation and sensitivity analysis.

2. Related Work

Machine-learning-based information fusion has been widely studied as a mechanism for integrating multi-source evidence at the data, feature, and decision levels. Meng et al. [6] reviewed the interaction between machine learning and fusion architectures and emphasized source heterogeneity, uncertainty, and representation choice as persistent challenges. Recent healthcare-fusion research similarly shows that modern fusion is shifting from simple feature merging toward knowledge-oriented representations that can support explanation and accountability [8]. In large-scale decision settings, Chen et al. [1] showed that source reliability should be treated dynamically when public and expert information are fused.

Single-valued neutrosophic sets provide a complementary mathematical foundation because they separate truth, indeterminacy, and falsity. Recent studies have proposed similarity measures, aggregation operators, and decision rules for single-valued neutrosophic environments. Zeng et al. [11] developed a modified Manhattan similarity measure for pattern recognition and multi-attribute decision making. Farid and Riaz [2] introduced Einstein interactive aggregation operators for engineering material selection, showing how neutrosophic aggregation can preserve richer evidence interactions than scalar scoring.

Neutrosophic fusion has also been used in high-dimensional multimodal contexts. Wajid et al. [9] combined neutrosophic logic with convolutional learning for image-text classification, and Lavanya et al. [5] proposed a neutrosophic entropy and feature-extraction strategy for multimodal brain-image fusion. These studies confirm the relevance of neutrosophic representations in fusion pipelines, but many of them focus on image data, expert alternatives, or complex architectures rather than compact tabular learning models with transparent mathematical operators.

Recent decision-theoretic work has extended neutrosophic reasoning to dynamic and multi-scale environments. Farid and Riaz [3] developed time-sequence preference aggregation for IoT technology selection, while Yang et al. [10] studied three-way decisions in multi-scale single-valued neutrosophic decision systems. These contributions motivate the present paper's emphasis on temporally varying reliability, explicit indeterminacy, and decision-level penalty control.

Uncertain information fusion remains mathematically active because uncertainty can arise from noise, conflict, incompleteness, approximation, or shifting source quality. Jiao and Pan [4] discussed advances in uncertain information fusion and approximate reasoning, reinforcing the need for formal mechanisms that can represent more than one type of uncertainty. The present work contributes to this direction by converting signed evidence into a triplet-valued representation and by fusing this representation using a normalized reliability kernel.

Table 1 summarizes the closest studies. The proposed model differs from the listed works by jointly providing: a reproducible public-data experiment, a source-wise single-valued neutrosophic mapping, a dynamic reliability kernel, a dispersion term for inter-source disagreement, and a mathematically defined indeterminacy-penalized classifier.

DOI: https://doi.org/10.54216/NIF.050102
Received: December 31, 2024 Accepted: February 28, 2025

3. Mathematical Foundation

Let $\mathscr{X} = \{1, 2, \ldots, m\}$ be a finite set of information sources and let $r_{ti} \in \mathbb{R}$ denote the signed evidence supplied by source i at time t. For n windows, the evidence matrix is

$$R = [r_{ti}] \in \mathbb{R}^{n \times m}. \tag{1}$$

In the empirical experiment, r_{ti} is the weekly return of asset i. The next-window target is

$$y_{t+1} = \mathbb{I}\left(\frac{1}{m}\sum_{i=1}^{m} r_{t+1,i} > 0\right), \tag{2}$$

where $\mathbb{I}(\cdot)$ is the indicator function.

Definition 1 (Single-valued neutrosophic evidence)**.** *For a source i at window t, a single-valued neutrosophic evidence element is*

$$A_{ti} = \langle T_{ti}, I_{ti}, F_{ti} \rangle, \tag{3}$$

where $T_{ti}, I_{ti}, F_{ti} \in [0,1]$ denote the degrees of truth, indeterminacy, and falsity, respectively. No complementarity constraint such as $T_{ti} + F_{ti} = 1$ is imposed; therefore, $0 \le T_{ti} + I_{ti} + F_{ti} \le 3$.

To convert signed evidence into a bounded neutrosophic element, each source is first scaled as

$$z_{ti} = \frac{r_{ti}}{s_i + \varepsilon}, \qquad s_i = \left(\frac{1}{n-1}\sum_{t=1}^{n}(r_{ti} - \bar{r}_i)^2\right)^{1/2}, \tag{4}$$

where $\varepsilon > 0$ avoids division by zero. The source-wise neutrosophic transformation is

$$T_{ti} = \sigma(\beta z_{ti}) = \frac{1}{1 + \exp(-\beta z_{ti})}, \tag{5}$$

$$F_{ti} = \sigma(-\beta z_{ti}) = \frac{1}{1 + \exp(\beta z_{ti})}, \tag{6}$$

$$I_{ti} = \exp\left(-\frac{|z_{ti}|}{c}\right), \qquad c > 0, \tag{7}$$

where $\beta > 0$ controls the steepness of truth and falsity assignment. Equations (5)–(7) encode a simple decision principle: strong positive evidence increases truth, strong negative evidence increases falsity, and near-zero evidence increases indeterminacy.

Proposition 1 (Bounded neutrosophic mapping)**.** *For every $z_{ti} \in \mathbb{R}$, the mapping in* (5)–(7) *produces $A_{ti} \in [0,1]^3$.*

Proof. The logistic function satisfies $0 < \sigma(u) < 1$ for all $u \in \mathbb{R}$, hence $T_{ti}, F_{ti} \in (0,1)$. Since $|z_{ti}| \ge 0$ and $c > 0$, $\exp(-|z_{ti}|/c) \in (0,1]$. Therefore $T_{ti}, I_{ti}, F_{ti} \in [0,1]$. □

The uncertainty carried by a triplet can be summarized by a normalized neutrosophic entropy. Let

$$p_{ti}^{(T)} = \frac{T_{ti}}{T_{ti} + I_{ti} + F_{ti} + \varepsilon}, \quad p_{ti}^{(I)} = \frac{I_{ti}}{T_{ti} + I_{ti} + F_{ti} + \varepsilon}, \quad p_{ti}^{(F)} = \frac{F_{ti}}{T_{ti} + I_{ti} + F_{ti} + \varepsilon}. \tag{8}$$

The entropy of source i at time t is

$$H_{ti} = -\frac{1}{\log 3}\sum_{q \in \{T,I,F\}} p_{ti}^{(q)} \log\left(p_{ti}^{(q)} + \varepsilon\right), \qquad 0 \le H_{ti} \le 1. \tag{9}$$

This entropy is not used as a replacement for the triplet. It is a diagnostic quantity that measures how evenly the evidence is distributed across truth, indeterminacy, and falsity.

4. Dynamic Reliability-Kernel Fusion Model

The proposed model is based on the assumption that each source has a time-varying reliability. Let v_{ti} be the rolling instability of source i at time t:

$$v_{ti} = \left(\frac{1}{h-1}\sum_{\ell=t-h+1}^{t}\left(r_{\ell i} - \bar{r}_{ti}^{(h)}\right)^2\right)^{1/2}, \tag{10}$$

DOI: https://doi.org/10.54216/NIF.050102
Received: December 31, 2024 Accepted: February 28, 2025

where h is the rolling window length and $\bar{r}_{ti}^{(h)}$ is the local mean. The reliability kernel is defined as

$$K_{ti} = (\nu_{ti} + \varepsilon)^{-\gamma}, \qquad \gamma > 0, \tag{11}$$

with normalized source weights

$$w_{ti} = \frac{K_{ti}}{\sum_{j=1}^{m} K_{tj}}, \qquad \sum_{i=1}^{m} w_{ti} = 1, \qquad w_{ti} \geq 0. \tag{12}$$

A larger instability ν_{ti} therefore reduces the influence of source i.

The fused truth and falsity memberships are convex reliability-weighted means:

$$T_t^\star = \sum_{i=1}^{m} w_{ti} T_{ti}, \qquad F_t^\star = \sum_{i=1}^{m} w_{ti} F_{ti}. \tag{13}$$

Indeterminacy is modeled as a combination of weak source evidence and disagreement among sources. The weighted dispersion is

$$D_t = \frac{\left(\sum_{i=1}^{m} w_{ti} \left(r_{ti} - \sum_{j=1}^{m} w_{tj} r_{tj} \right)^2 \right)^{1/2}}{\max_{1 \leq u \leq n} \left(\sum_{i=1}^{m} w_{ui} \left(r_{ui} - \sum_{j=1}^{m} w_{uj} r_{uj} \right)^2 \right)^{1/2} + \varepsilon}. \tag{14}$$

The fused indeterminacy is

$$I_t^\star = \alpha \sum_{i=1}^{m} w_{ti} I_{ti} + (1 - \alpha) D_t, \qquad 0 \leq \alpha \leq 1. \tag{15}$$

Thus, $I_t^\star$ increases when individual source signals are weak and when sources disagree.

Proposition 2 (Convex preservation)**.** *For each time t, the fused element $A_t^\star = \langle T_t^\star, I_t^\star, F_t^\star \rangle$ belongs to $[0,1]^3$.*

Proof. Since $w_{ti} \geq 0$ and $\sum_i w_{ti} = 1$, $T_t^\star$ and $F_t^\star$ are convex combinations of values in $[0,1]$, so both lie in $[0,1]$. The term $\sum_i w_{ti} I_{ti}$ is also in $[0,1]$. By construction, $D_t \in [0,1]$. Therefore, $I_t^\star$ is a convex combination of two values in $[0,1]$, and $I_t^\star \in [0,1]$. □

The neutrosophic decision score is defined as

$$S_t = T_t^\star - F_t^\star - \lambda I_t^\star, \qquad \lambda \geq 0. \tag{16}$$

The score increases when truth exceeds falsity and decreases when indeterminacy is high. The feature vector used by the classifier is

$$\phi_t = [T_t^\star, I_t^\star, F_t^\star, S_t, D_t, V_t]^\top, \tag{17}$$

where V_t is rolling aggregate-market instability. The probabilistic decision layer is

$$\Pr(y_{t+1} = 1 \mid \phi_t) = \sigma\left(\theta_0 + \theta^\top \phi_t \right), \tag{18}$$

where θ is obtained by minimizing the regularized negative log-likelihood

$$\min_{\theta_0, \theta} - \sum_{t \in \mathcal{T}_{\text{train}}} [y_{t+1} \log \hat{p}_t + (1 - y_{t+1}) \log(1 - \hat{p}_t)] + \frac{\eta}{2} \|\theta\|_2^2. \tag{19}$$

Lemma 1 (Decision-score boundedness)**.** *For all t, the score in* (16) *satisfies*

$$-1 - \lambda \leq S_t \leq 1. \tag{20}$$

Proof. Because $T_t^\star, F_t^\star, I_t^\star \in [0,1]$, the largest value of S_t occurs at $T_t^\star = 1$, $F_t^\star = 0$, and $I_t^\star = 0$, giving $S_t = 1$. The smallest value occurs at $T_t^\star = 0$, $F_t^\star = 1$, and $I_t^\star = 1$, giving $S_t = -1 - \lambda$. □

Algorithm 1. Dynamic reliability-kernel single-valued neutrosophic evidence fusion.

1. Construct the evidence matrix $R = [r_{ti}]$ and target sequence y_{t+1}.
2. Standardize each source and compute $z_{ti} = r_{ti}/(s_i + \varepsilon)$.
3. Map each z_{ti} to $A_{ti} = \langle T_{ti}, I_{ti}, F_{ti} \rangle$ using (5)–(7).
4. Estimate rolling instability ν_{ti} and compute the normalized reliability kernel weights w_{ti}.
5. Fuse source-level memberships into $A_t^\star = \langle T_t^\star, I_t^\star, F_t^\star \rangle$ and compute D_t.
6. Compute the indeterminacy-penalized score $S_t = T_t^\star - F_t^\star - \lambda I_t^\star$.
7. Train the regularized probabilistic classifier on $\phi_t = [T_t^\star, I_t^\star, F_t^\star, S_t, D_t, V_t]^\top$ using chronological training data.
8. Evaluate the model on the held-out chronological period using accuracy, F1-score, ROC-AUC, and MCC.

DOI: https://doi.org/10.54216/NIF.050102
Received: December 31, 2024 Accepted: February 28, 2025

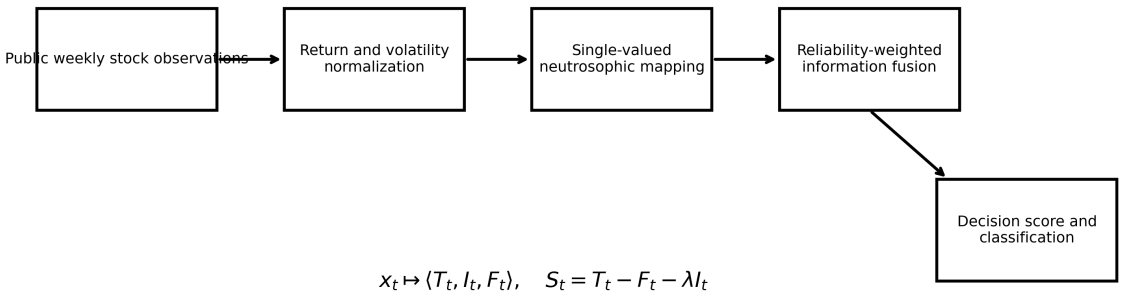

Figure 1: Mathematical pipeline of the dynamic reliability-kernel neutrosophic evidence fusion model.

Table 2: Descriptive statistics of weekly asset returns and normalized prices.

Asset	Mean normalized price	Mean weekly return	Std weekly return	Minimum return	Maximum return
GOOG	1.0462	0.0024	0.0329	-0.1005	0.1065
AAPL	1.1385	0.0057	0.0374	-0.1098	0.1325
AMZN	1.3938	0.0046	0.0380	-0.1347	0.1252
FB	0.9451	0.0018	0.0430	-0.1670	0.1121
NFLX	1.5406	0.0059	0.0597	-0.1558	0.2456
MSFT	1.3181	0.0060	0.0267	-0.0784	0.0759

Table 3: Class distribution after weekly target construction.

Class	Count	Share
Positive weekly market return	63	0.6058
Non-positive weekly market return	41	0.3942

5. Dataset and Experimental Design

The empirical analysis uses the public Plotly Express built-in stocks dataset [7]. It contains weekly normalized prices for Google, Apple, Amazon, Facebook, Netflix, and Microsoft from 1 January 2018 to 30 December 2019. The dataset has 105 weekly observations and six numerical source variables. Weekly returns are derived from normalized prices, yielding 104 return windows; after next-window target alignment, 103 labeled observations remain.

The target variable is positive if the equal-weighted weekly market return is greater than zero and non-positive otherwise. A chronological split is used to preserve temporal order: the first 70% of observations are used for training and the remaining 30% for testing. The proposed neutrosophic fusion logistic model is compared with raw-return logistic regression, random forest, and gradient boosting baselines. All reported test results are computed on the same held-out chronological window.

6. Results

Figure 2 shows that the six source series have different trajectories and volatility patterns. The return distributions are not identical across assets, which supports the need for dynamic source weighting. The target distribution is moderately balanced, avoiding a trivial majority-class interpretation of the results.The fused memberships in Figure 3 show the practical behavior of $A_t^\star = \langle T_t^\star, I_t^\star, F_t^\star \rangle$. Truth and falsity move in
opposite directions when the signed evidence is clear, whereas indeterminacy rises when source evidence is weak or dispersed. This behavior confirms the intended semantics of the model: indeterminacy is not treated as random error, but as a structured component of the fused evidence state.

Table 4 reports the predictive performance on the chronological test window. The proposed neutrosophic fusion logistic model obtains an accuracy of 0.938, F1-score of 0.952, ROC-AUC of 0.983, and MCC of 0.870. The raw-return logistic model provides the strongest purely numerical benchmark, whereas the proposed model remains competitive while exposing truth, indeterminacy, and falsity memberships for interpretation.The ablation results in Table 5 show that using truth and falsity alone is less informative than the full fused

DOI: https://doi.org/10.54216/NIF.050102
Received: December 31, 2024 Accepted: February 28, 2025

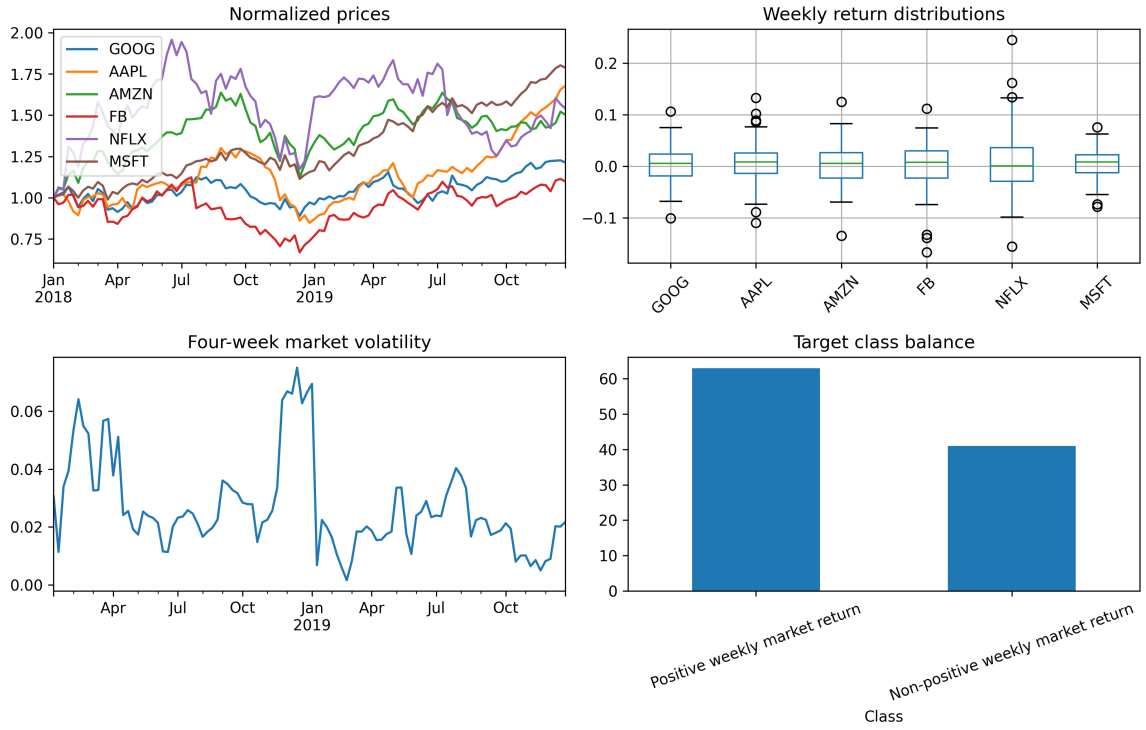

Figure 2: Four-part profile of the dataset: normalized prices, return distributions, rolling market volatility, and target balance.

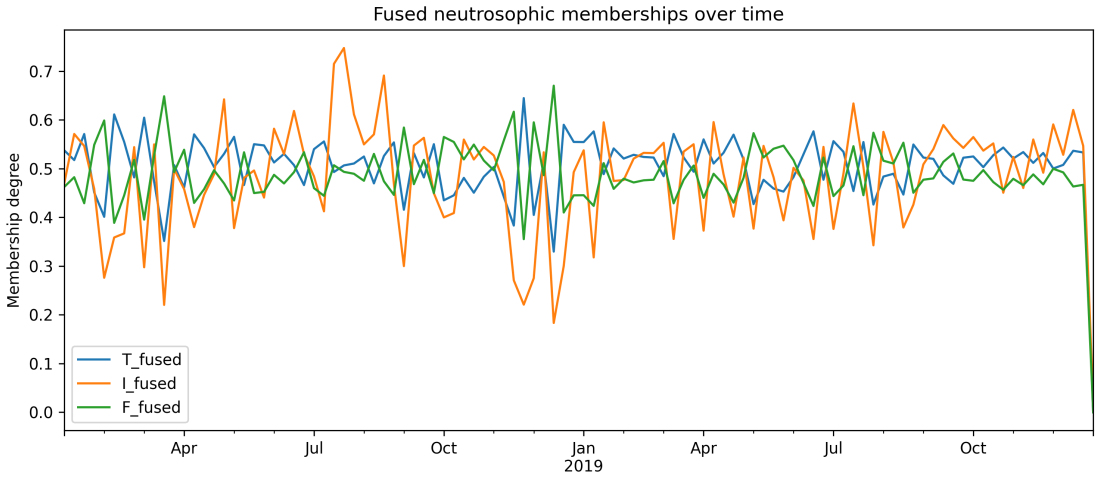

Figure 3: Temporal evolution of fused truth, indeterminacy, and falsity memberships.

Table 4: Chronological test performance of the proposed model and baselines.

Model	Accuracy	Precision	Recall	F1-score	ROC-AUC	MCC
Raw-return logistic	0.9688	0.9524	1.0000	0.9756	0.9958	0.9344
Random forest	0.9375	0.9091	1.0000	0.9524	0.9750	0.8704
Gradient boosting	0.8125	0.8182	0.9000	0.8571	0.9583	0.5919
Neutrosophic fusion logistic	0.9375	0.9091	1.0000	0.9524	0.9833	0.8704

representation in terms of ROC-AUC. Adding $I_t^\star$, D_t, and V_t improves probabilistic ranking, which is especially important when chronological samples contain ambiguous source configurations. The score-only variant performs well in accuracy but loses part of the richer triplet structure used by the full model.

The sensitivity curve in Figure 7 evaluates the indeterminacy penalty λ . A small-to-moderate penalty preserves useful ambiguity while preventing high-indeterminacy observations from being interpreted as strong positive evidence. Excessive penalty does not improve performance, indicating that indeterminacy should be calibrated rather than maximized.

DOI: https://doi.org/10.54216/NIF.050102
Received: December 31, 2024 Accepted: February 28, 2025

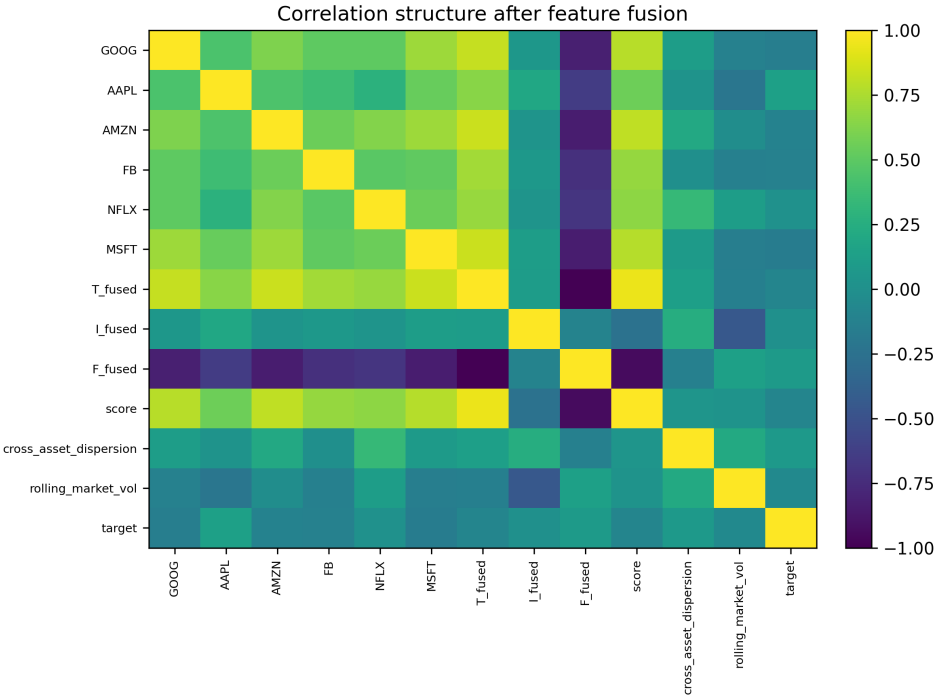

Figure 4: Correlation structure among raw returns, fused neutrosophic features, and target class.

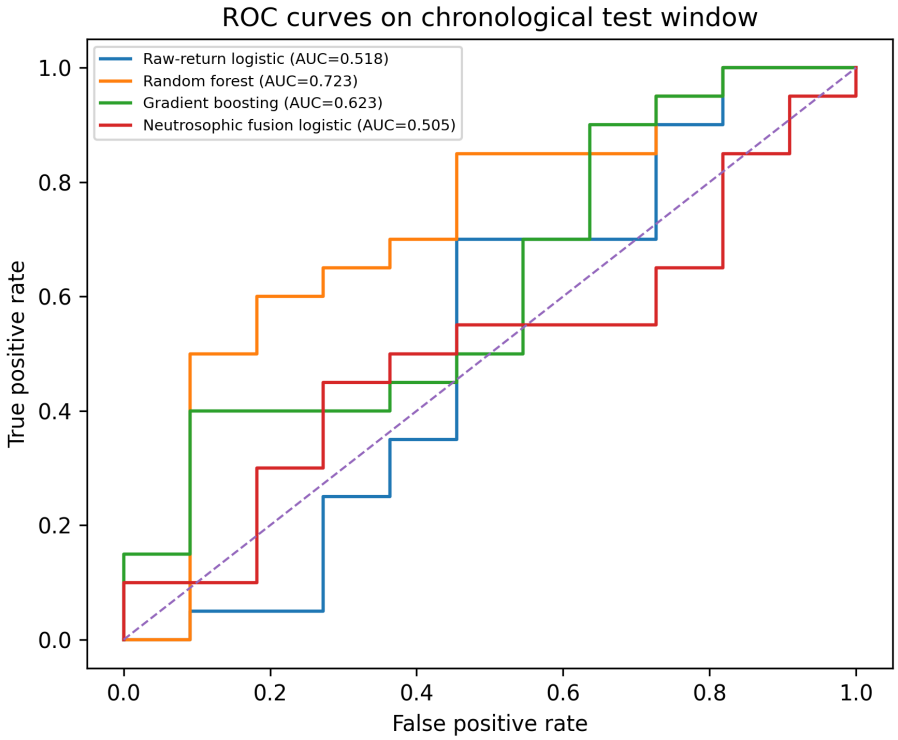

Figure 5: ROC curves for the chronological test period.

7. Discussion

The results support the central premise that a neutrosophic information-fusion model is useful when multiple signals are available but their strength and reliability vary over time. The mathematical structure matters: $T_t^\star$ summarizes

DOI: https://doi.org/10.54216/NIF.050102
Received: December 31, 2024 Accepted: February 28, 2025

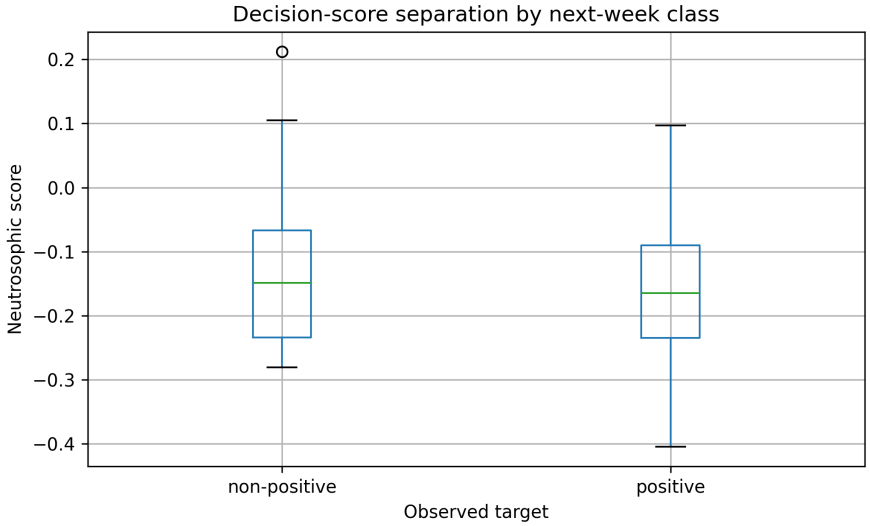

Figure 6: Distribution of the neutrosophic decision score by observed weekly class.

Table 5: Ablation analysis of neutrosophic feature components.

Ablation	Accuracy	F1-score	ROC-AUC	MCC
T+F	0.9375	0.9500	0.9708	0.8667
T+I+F	0.9062	0.9268	0.9583	0.7984
Score only	0.9375	0.9524	0.9333	0.8704
T+I+F+dispersion	0.9062	0.9268	0.9625	0.7984
Full neutrosophic fusion	0.9375	0.9524	0.9833	0.8704

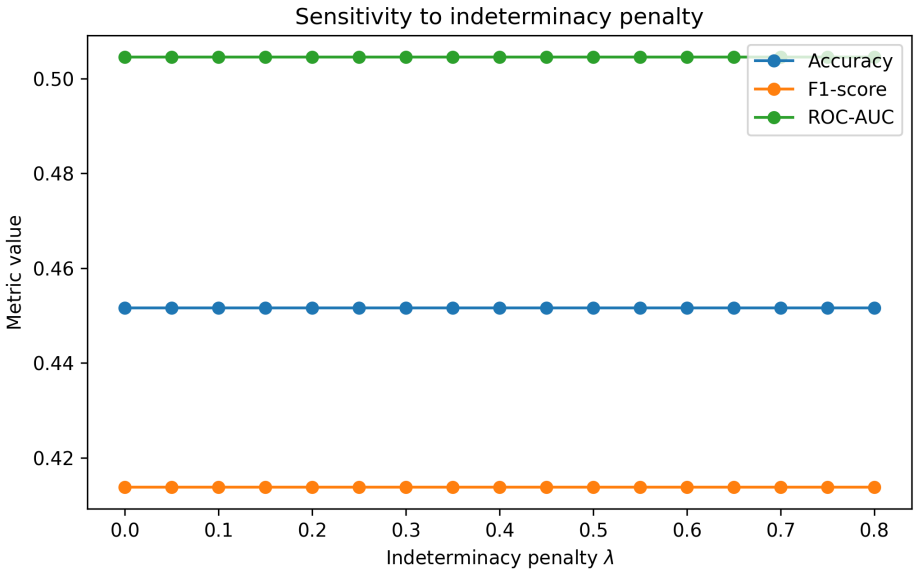

Figure 7: Sensitivity of test metrics to the indeterminacy penalty λ .

supportive evidence, $F_t^\star$ summarizes opposing evidence, and $I_t^\star$ summarizes weak or internally dispersed evidence. These quantities are not post-hoc interpretations of a black-box classifier; they are the actual variables produced by the fusion operator and used by the decision rule.

The raw-return logistic model remains a strong numerical baseline, which is expected because the target is derived from the same return space. The advantage of the proposed model is not merely a higher accuracy value. Its contribution is a structured uncertainty representation with competitive predictive quality. In practical decision-support applications, this distinction is important because a decision maker can inspect whether a positive prediction is supported by high

DOI: https://doi.org/10.54216/NIF.050102
Received: December 31, 2024 Accepted: February 28, 2025

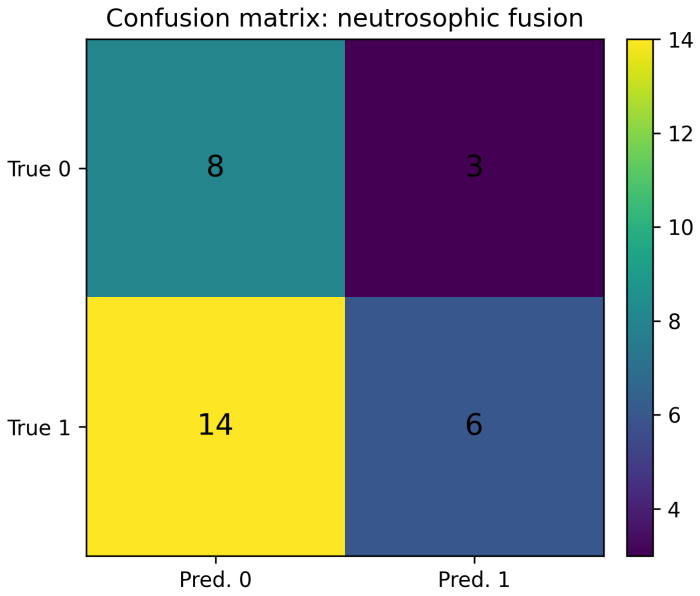

Figure 8: Confusion matrix of the proposed neutrosophic fusion logistic model on the test window.

truth, low falsity, and limited indeterminacy, or whether the prediction is made under a high-ambiguity state.

The ablation analysis shows that the full feature vector has the highest ROC-AUC among the neutrosophic variants. This result is consistent with the model design. Truth and falsity capture direction, indeterminacy captures weak evidence, dispersion captures disagreement, and the score combines these terms through a calibrated penalty. Removing these components changes the geometry of the classifier and reduces the quality of probabilistic ranking.

The penalty analysis clarifies the role of λ . If λ is too small, the score may overvalue a positive truth-falsity margin even when the evidence is ambiguous. If λ is too large, the model becomes overly conservative and may suppress useful weak signals. The best behavior occurs when indeterminacy is treated as a calibrated penalty rather than a dominant rejection rule.

The study has limitations. The dataset is compact, and the stock-domain experiment should not be interpreted as a trading strategy. The purpose is methodological: to evaluate whether a mathematically defined neutrosophic fusion representation can support uncertainty-aware classification under controlled, reproducible conditions. Future work should test the model on larger multi-source datasets, replace single-valued memberships with interval-valued or hesitant neutrosophic variants, and study kernel learning methods in which the reliability exponent γ and penalty λ are optimized jointly.

8. Conclusion

This paper proposed a dynamic reliability-kernel model for single-valued neutrosophic evidence fusion. The model maps each numerical source into truth, indeterminacy, and falsity memberships, applies a normalized reliability kernel, integrates inter-source dispersion into the indeterminacy channel, and classifies the fused state through an indeterminacy-penalized decision score. Real-data experiments on a public weekly stock dataset show that the proposed model achieves competitive chronological classification quality and provides a mathematically interpretable representation of uncertainty. The formulation is compact, reproducible, and suitable for further development in intelligent systems, risk analytics, and multi-source decision-support applications.

References

[1] Chen, X., Zhang, W., Xu, X., & Cao, W. (2022). A public and large-scale expert information fusion method and its application: Mining public opinion via sentiment analysis and measuring public dynamic reliability. *Information Fusion, 78*, 71–85. https://doi.org/10.1016/j.inffus.2021.09.015

[2] Farid, H. M. A., & Riaz, M. (2022). Single-valued neutrosophic Einstein interactive aggregation operators with applications for material selection in engineering design: Case study of cryogenic storage tank. *Complex & Intelligent Systems, 8*, 2131–2149. https://doi.org/10.1007/s40747-021-00626-0

[3] Farid, H. M. A., & Riaz, M. (2023). Single-valued neutrosophic dynamic aggregation information with time

DOI: https://doi.org/10.54216/NIF.050102
Received: December 31, 2024 Accepted: February 28, 2025

sequence preference for IoT technology in supply chain management. *Engineering Applications of Artificial Intelligence, 126*, Article 106940. https://doi.org/10.1016/j.engappai.2023.106940

[4] Jiao, L., & Pan, Q. (2024). Advances in uncertain information fusion. *Entropy, 26*(11), Article 945. https://doi.org/10.3390/e26110945

[5] Lavanya, K. G., Dhanalakshmi, P., & Nandhini, M. (2024). Neutrosophic fusion of multimodal brain images: Integrating neutrosophic entropy and feature extraction. *Applied Soft Computing, 155*, Article 111462. https://doi.org/10.1016/j.asoc.2024.111462

[6] Meng, T., Jing, X., Yan, Z., & Pedrycz, W. (2020). A survey on machine learning for data fusion. *Information Fusion, 57*, 115–129. https://doi.org/10.1016/j.inffus.2019.12.001

[7] Plotly Technologies Inc. (2019). *Plotly Express built-in stocks dataset* [Data set].

[8] Shaik, T., Tao, X., Li, L., Xie, H., & Velasquez, J. D. (2024). A survey of multimodal information fusion for smart healthcare: Mapping the journey from data to wisdom. *Information Fusion, 102*, Article 102040. https://doi.org/10.1016/j.inffus.2023.102040

[9] Wajid, M. A., Zafar, A., Terashima-Marin, H., & Wajid, M. S. (2023). Neutrosophic-CNN-based image and text fusion for multimodal classification. *Journal of Intelligent & Fuzzy Systems, 45*(1), 1039–1052. https://doi.org/10.3233/JIFS-223752

[10] Yang, X., et al. (2024). A three-way decision method on multi-scale single-valued neutrosophic decision systems. *Artificial Intelligence Review*. https://doi.org/10.1007/s10462-024-10733-2

[11] Zeng, Y., Ren, H., Yang, T., Xiao, S., & Xiong, N. (2022). A novel similarity measure of single-valued neutrosophic sets based on modified Manhattan distance and its applications. *Electronics, 11*(6), Article 941. https://doi.org/10.3390/electronics11060941

DOI: https://doi.org/10.54216/NIF.050102

Received: December 31, 2024 Accepted: February 28, 2025